

COMBUSTION TUBE SOOT FROM A DIESEL FUEL/AIR MIXTURE

L. B. Ebert and J. C. Scanlon

Exxon Research and Engineering; Annandale, NJ 08801

C. A. Clausen

University of Central Florida; Orlando, FL 32816

INTRODUCTION

Used by the Chinese to make inks many years before Christ (1), soot was an environmental nuisance by the time of the industrial revolution (2). Today, soot can be both useful (the carbon black industry) and detrimental (diesel exhaust), so that investigations of soot can impact wide-ranging areas. Curiously, although there is intuitive understanding about the commonality of soots from a variety of sources, including furnace flames, piston engines, combustion chambers, or premixed flames (2), there is no general agreement about the detailed molecular structure of soot. Recently, Zhang, O'Brien, Heath, Liu, Curl, Kroto, and Smalley (ZOHLCKS) proposed to interrelate soot with carbon clusters of icosahedral symmetry (3). They suggested that "the polycyclic aromatic molecules known to be present in high concentrations in sooting flames may therefore adopt pentagonal rings as they grow, so as to generate spheroidal structures which maximize the number of C-C linkages," ultimately yielding a soot nucleus consisting of "concentric, but slightly imperfect spheres" (3). Thus, ZOHLCKS proposed that the spherical morphology of soot particles arose from soot "molecules" of nearly spherical symmetry.

In this paper, we discuss the structural and chemical characterization of soot formed in a combustion tube, in part to address the ZOHLCKS proposal, in part to develop information to compare soot to a variety of other carbonaceous materials.

EXPERIMENTAL DETAILS

Samples of soot were generated at the University of Central Florida by the combination of no. 2 diesel fuel (C-13 NMR aromaticity 19%) with air in a combustion tube of inner diameter 9.8 cm. Sample 1 was generated by injecting the air and fuel (at a mass ratio of 5:1) preheated to 75°C into the combustion tube heated to 1150°C. For sample 2, the combination of air preheated to 600°C with diesel fuel preheated to 350°C in an unheated combustion tube led to spontaneous ignition. The combustion process was allowed to proceed under basically adiabatic conditions; the flame tem-

perature reached a maximum of $\sim 900^{\circ}\text{C}$. Further information on the diesel fuel is available (4).

X-ray diffraction was performed on a Siemens D-500 using copper radiation. Debye internal interference calculations were done as previously reported (5-7).

Elemental analysis of sample 2 was done by Galbraith. Duplicate runs made on carbon and hydrogen yielded average values of $\%C = 90.08$ (89.94, 90.21) and $\%H = 1.76$ (1.82, 1.69) for an average H/C atomic ratio of 0.23. The sample had 0.22%N (N/C= 0.002) and 4.64%O (O/C=0.04). Ash by thermogravimetric analysis was 0.19%.

Sample 2 was reacted with potassium naphthalene (~ 1) in tetrahydrofuran (THF) at room temperature. A solution of 30 minute old naphthalene radical ion (0.380 g, 2.97 mmol naphthalene in 25.810 g THF; with 2.498 g, 63.9 mmol K°) was added to 0.675 g sample 2. After 2 hours 15 minutes, there was a consumption of 0.404 g, 10.3 mmol K° , determined by weighing the solid K° ; that the total K° uptake of 10.3 mmol exceeded the amount of naphthalene (2.97 mmol) suggested that the deposit was reacting. After 23 hours 15 minutes, there was a consumption of 0.536 g, 13.7 mmol K° and the solution was quenched at 0°C with the addition of solution of 2.836 g CD_3I in 1.845 g THF. The solution was allowed to stand at room temperature under inert gas for 24 hours, and then was filtered through a medium porosity frit. Following drying, the entrained solids weighed 2.589 g; following rotary evaporation, the material which passed the filter weighed approximately 0.29 g. A Bruker MSL was used for D-2 in the solid state (55.283 MHz).

RESULTS AND DISCUSSION. X-RAY DIFFRACTION.

Figure 1 gives the diffraction pattern of sample 2 over the range $15 - 105^{\circ} 2\theta$ (Cu). There are four readily observed diffraction peaks, which fall into the range normally associated with the (002), (100), (004), and (110) peaks of graphite or other benzenoid arrays. There are no (hkl) peaks having non-zero hk and non-zero l (e.g., (101)), suggesting that the material is turbostratic, meaning that there is no well-defined registry between adjacent planes (as found in the ABAB stacking sequence of graphite). The most intense peak, the (002), arises from interference between approximately parallel aromatic entities, and thus gives information about aromatic stacking. Figure 2 shows that sample 1 and sample 2 have (002) peaks of different widths. Sample 1 has $d(002)$ at 3.63 Å of width 0.122 radians, corresponding to a crystallite size in the direction of aromatic stacking of 12 Å; sample 2 has $d(002)$ at 3.60 Å of width 0.070 radians, corresponding to a crystallite size of 20 Å. (Scherrer constant = 0.9).

The (100) and (110) diffraction peaks give information about the size of the benzenoid array. As given in Figure 3, the linewidths of these peaks suggest sizes of 22 to 28 Å, if one uses a Scherrer constant of 1.84. However, as pointed out by Warren and Bodenstein in a study of carbon blacks (8) and by Ergun (9), the use of the 1.84 constant can give unreliable results for in-plane crystallite sizes < 50 Å. For crystallite sizes near 20 Å (8), the Scherrer constant is about 1.4 for the (100) and about 1.6 for the (110), which then give us crystallite sizes of 21 Å (100) and 19 Å (110).

Knowledge of the lattice constants can allow us to predict microscopic density. For graphite, which has $a_c = 2.45$ Å (= C - C bond distance of $1.415 \text{ Å} \times \sqrt{3}$) and $c_c = 6.74$ Å, one obtains a unit cell volume of $(a_c^2)c_c \times 0.866 = 35.0 \text{ Å}^3$. This unit cell has four carbon atoms, so we have $8.76 \text{ Å}^3/\text{C}$ atom. This yields a predicted density of 2.28 gram/cm^3 . If we consider the effect of the different c_c of the soot on density (e.g., (002) at 3.60 Å instead of 3.37 Å), we calculate a unit volume of $9.36 \text{ Å}^3/\text{C}$ atom and a density of 2.13 gram/cm^3 . The changes associated with a_c are smaller, and in the other direction. Intuitively, and on the basis of the (100) peak, we would expect a limiting sp^2 - sp^2 bond distance of 1.39 Å, and correlative a_c of 2.41 Å. If we consider the effect of both the increased c_c and the possible decreased a_c on density, we find a volume of $9.05 \text{ Å}^3/\text{C}$ and a density of 2.21 gram/cm^3 . The key point from these calculations is that the increase in c_c found in the soot can change the predicted density only about 7%; this change is not enough to account for the observed densities of 1.8 to 2.0 gram/cm^3 typically found in soots (M. Frenklach, personal communication).

Having appreciable amounts of hydrogen, the soot is better viewed as a "large" polynuclear aromatic rather than as a "small" graphite. Because hydrogen-hydrogen and carbon-hydrogen interactions are key structural determinants for aromatic hydrocarbons, the densities are much lower for the aromatics than for graphite: naphthalene (1.145), anthracene (1.25), phenanthrene (1.182), biphenylene (1.24), pyrene (1.27), picene (1.324), perylene (1.341), and coronene (1.38). Relating observed density to wgt% carbon for the above aromatics, we obtain

$$\text{density} = 0.10814 (\%C) - 8.988 \quad R = .9546$$

If one extrapolated to graphite, using the densities of these hydrocarbons as a guide, one obtains a density of only 1.826.

What do we expect for a soot of spherical carbon clusters? One must consider effects due to intramolecular scattering (analogous to the (100) and (110) peaks in benzenoid

arrays) and due to intermolecular scattering (analogous to the (002) and (004) peaks in graphite).

For intramolecular interference, we have simulated the scattering from one truncated icosahedron of bond length 1.54 Å using the formalism of Debye internal interference, and the results are given in Figure 4. In the figure, the x axis is linear in k , with $k = 2\pi/d = 4\pi\sin\theta/\lambda$ (θ = Bragg angle, λ = wavelength of x-radiation), and one sees two peaks in the range $k = 0.8$ to 2.8 , neither of which are observed in our soot. As one changes the bond length of the icosahedron, one will change the peak maxima in a predictable way, with the coefficient relating bond length to d value given by the Miller index of the peak (5,6). For instance, for the (002) peak in a stack of seven parallel coronene molecules, changing the interplanar spacing from 3.20 Å to 3.95 Å changes the observed d value from 3.16 Å to 3.87 Å (5, 6).

For intermolecular interference between spheroids, let us assume that we can place all carbon atoms on the surface of one spheroid at a distance of ca. 3.6 Å from carbon atoms of some other spheroid. In this way, we can get a "(002)" peak at 3.6 Å, as observed in the soot, but one notes that the linewidth of such a peak will correspond only to a "stack" of two aromatics (crystallite size ca. 7.2 Å). If one goes to the concentric shell model (Figure 4 of ref. 3), one can obtain a larger apparent stack height; to account for the data on sample 2, one would need 5 to 6 shells (20 Å/3.6 Å) to obtain the observed (002) linewidth. Such an entity would have a large fraction of non-protonated (quaternary) aromatic carbon atoms, just as graphite does, and, from a chemical point of view, would be more like graphite than aromatic hydrocarbons. To address this more fully, we performed chemical experiments on sample 2.

BACKGROUND. CHEMICAL REDUCTION.

The use of potassium naphthalene (-1) in THF to reduce fossil fuel materials has been reviewed by Stock (10) and by Ebert (11). If one wants to distinguish graphite-like chemistry from polynuclear aromatic hydrocarbon chemistry, reduction by naphthalene (-1) followed by alkylation by alkyl iodide is useful because different products are obtained. Graphite is reduced by naphthalene (-1) and correlatively intercalated by K^+ and THF; the potassium intercalate is not alkylated by alkyl iodides. Aromatic hydrocarbons of reduction potential less negative than the -2.5 V (vs. SCE) of naphthalene (-1) will be reduced to anions, which can then (usually) be alkylated by alkyl iodides to give products in which the alkyl group is attached to an sp^3 -hybridized carbon of the reduced aromatic.

With respect to the reduction, there has been a belief in the literature that aromatic hydrocarbons can form numer-

ous highly charged poly-anions driven by the presence of excess alkali metal. Examples include the dianion of naphthalene (10) and tetraanions of pyrene and perylene. Noting that the difference in reduction potential between the radical anion and dianion of anthracene is 0.48 V (12), one would expect the dianion of naphthalene to have a reduction potential of at least -2.98 V (vs. SCE), near that of K^0 itself; we are unaware of any work in which a second reduction peak has been measured for naphthalene and in fact with pyrene third and fourth reduction peaks are not seen (13).

Relevant to the shell proposal for soot of ZOHLCKS (3), Stock proposed that the reductive alkylation of coal suggested a model "in which molecular fragments of coal are peeled away from the solid as layers from an onion" (10). To address this, we performed reductive methylation (with CD_3I) of Burning Star coal to determine if methyl groups added preferentially to the "soluble" phase (14). The coal consumed 10.4 mmol K/g , and, following alkylation, 52% of the product carbon was in the "THF-soluble" phase and 48% in the "THF-insoluble" phase. Solid state 2D NMR showed CD_3 groups in both phases, with the THF-soluble phase having only 87% of the deuterium of the insoluble phase, on a per carbon atom basis! The spectrum of the insolubles showed only a first order quadrupole split spectrum (separation = 51.7 G, indicative of three-fold rotation of bound $-CD_3$ groups) but the solubles showed a strong (averaged) central peak and a quadrupolar split line. Significantly, these results for coal, which are those expected for alkylation of aromatics and heterocyclics, are similar to what we report here for soot.

RESULTS AND DISCUSSION. REDUCTIVE ALKYLATION.

At 23 hours 15 minutes, the soot took up 15.9 mmol $K/gram$, correcting for consumption of potassium by naphthalene(-1). Figures 5 and 6 give the 2D NMR of the solid solubles and insolubles, and we see that the soot has behaved like a polynuclear aromatic in being alkylated by CD_3I . Figure 7 gives the 2D NMR of the solubles in methylene chloride, showing CD_3 groups bound primarily to sp^3 carbon, as expected for the reductive alkylation of polynuclear aromatics (15); some methylation of oxygen does occur.

One might be concerned with contamination of the THF-soluble sample by vast amounts of 1,4 dimethyl 1,4 dihydro naphthalene. Actually, naphthalene (-1) reduces methyl iodide to methyl radicals, in contrast to anions of larger aromatics which do in fact undergo alkylation (15, 16). Analysis of the THF-solubles by GC/MS, with quantification by flame ionization detection, shows the ratio of naphthalene to the most abundant dimethyl dihydro naphthalene to be 19.7/1; this is consistent with solution phase ^{13}C NMR which

shows three sharp aromatic peaks at 125.7, 127.7, and 133.3 δ , the shift positions of naphthalene itself. The underlying aromatic envelope goes from 120 to 146 δ , and there are aliphatic peaks at 14.2, 22.8, 25.9, 29.4, 29.7, 30.09, 30.34, 31.98, 34.26, and 37.46 δ . Aliphatic carbon bound to oxygen is suggested by a peak at 68 δ .

In conclusion, we see that the soot anion, in being alkylated by CD₁, behaves as anions of larger polynuclear aromatics, such as perylene and decacyclene (16) and not like the anion of graphite with K⁺. Naphthalene, with excess K⁺, behaves as naphthalene (-1).

Acknowledgements--We thank Mike Matturro for giving us the atomic coordinates of the 60 atom truncated icosahedron, Rod Kastrop for for the high resolution NMR spectra, and Manny Garcia for the D-2 NMR of solid samples.

REFERENCES

1. Y. Schwob, Chem. Phys. Carbon, 15, 109 (1979).
2. H. GG. Wagner, 17th Symposium on Combustion, pp. 3-19 (1978).
3. Q. L. Zhang, S. C. O'Brien, J. R. Heath, Y. Liu, R. F. Curl, H. W. Kroto, and R. E. Smalley, J. Phys. Chem., 90, 525 (1986).
4. Oak Ridge National Laboratory report ORNL/TM-9196 (November 1983).
5. L. B. Ebert, J. C. Scanlon, and D. R. Mills, Preprints, Petroleum Division of the Amer. Chem. Soc., 28(5), 1353 (1983).
6. _____, Liq. Fuels Technology, 2, 257 (1984).
7. _____, Preprints, Petroleum Division of the Amer. Chem. Soc., 30(4), 636 (1985).
8. B. E. Warren and P. Bodenstein, Acta Cryst., 18, 282 (1965).
9. S. Ergun, Chem. Phys. Carbon, 3, 211 (1968).
10. L. M. Stock, in Coal Science, Academic, 1982, pp. 161-282.
11. L. B. Ebert, in Chemistry of Engine Combustion Deposits, Plenum, 1985, pp. 303-376.
12. A. J. Bard and L. R. Faulkner, Electrochemical Methods, Wiley, 1980, p. 701.
13. J. Mortensen and J. Heinze, Tet. Lett., 26, 415 (1985).
14. A. R. Garcia, L. B. Ebert, and B. G. Silbernagel, Extended Abstracts of the 18th Biennial Carbon Conference, July, 1987.
15. L. B. Ebert, G. E. Milliman, D. R. Mills, and J. C. Scanlon, in Advances in Chemistry Series No. 217 (Polynuclear Aromatic Hydrocarbons), Amer. Chem. Soc., 1987.
16. L. B. Ebert, D. R. Mills, and J. C. Scanlon, Preprints, Petroleum Division of the Amer. Chem. Soc., 32(2), 419 (1987).

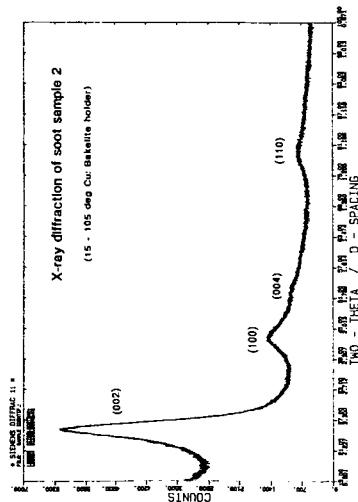


Figure 1. X-ray diffraction of sample 2.

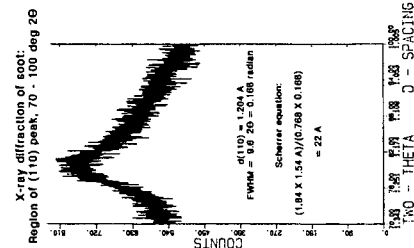
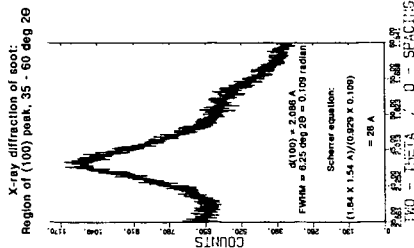


Figure 3. X-ray diffraction: (100) and (110) of sample 2

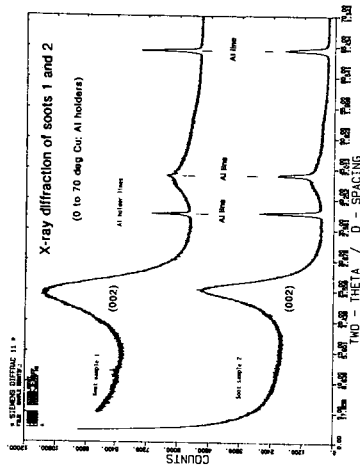


Figure 2. X-ray diffraction comparison: 1 vs. 2.

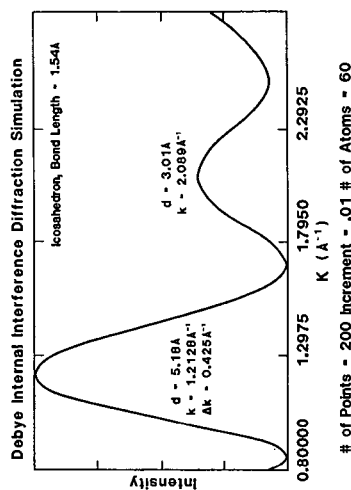


Figure 4. X-ray diffraction simulation: truncated icosahedron

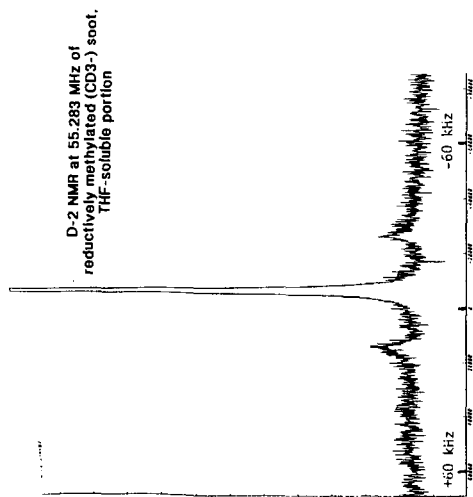


Figure 5. D-2 NMR of Me-soot THF-solubles

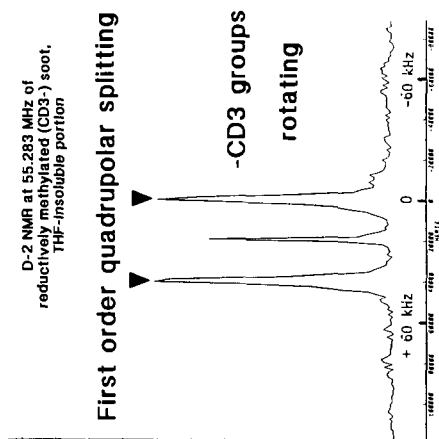


Figure 6. D-2 NMR of Me-soot THF-insolubles

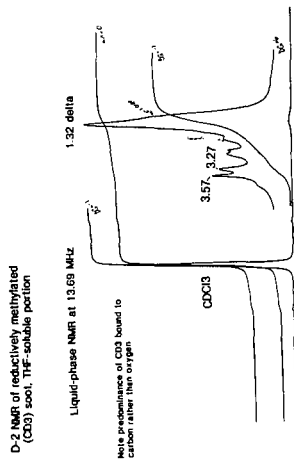


Figure 7. High resolution D-2 NMR of THF-sol